models were refined by full-matrix least-squares procedures. All non-hydrogen atoms were made anisotropic for **2a** and **2a**$^+$; in the case of **1a** this was done only for the atoms within the coordination sphere. Hydrogen atoms were included at their idealized positions and were refined isotropically with fixed thermal parameters. The final convergent refinement gave residuals as summarized in Table VII. The highest difference Fourier peaks were 0.56, 1.64, and 1.17 e Å^{-3} near the metal atom for **1a**, **2a**, and **2a**$^+$, respectively. Atomic coordinates and isotropic thermal parameters for the three structures are collected in Tables VIII–X.

Acknowledgment. We are grateful to the Department of Science and Technology, New Delhi, for establishing a National Single Crystal Diffractometer Facility at the Department of Inorganic Chemistry, Indian Association for the Cultivation of Science. Financial support received from the Council of Scientific and Industrial Research is also acknowledged.

Supplementary Material Available: Listings of anisotropic thermal parameters (Tables XI, XVI, and XXI), complete bond distances (Tables XII, XVII, and XXII) and angles (Tables XIII, XVIII, and XXIII), hydrogen atom positional parameters (Tables XIV, XIX, and XXIV), and structure determination summaries (Tables XV, XX, and XXV) for *cis*-$Os(Mex)_2(PPh_3)_2$, *trans*-$Os(Mex)_2(PPh_3)_2$, and *trans*-$[Os(Mex)_2(PPh_3)_2]PF_6 \cdot 2H_2O$, respectively (18 pages); listings of observed and calculated structure factors for the above three complexes (59 pages). Ordering information is given on any current masthead page.

Contribution from the Solar Energy Research Institute, Golden, Colorado 80401, and Department of Chemistry and Biochemistry, University of Colorado, Boulder, Colorado 80309

Relationship between the Bite Size of Diphosphine Ligands and Tetrahedral Distortions of "Square-Planar" Nickel(II) Complexes: Stabilization of Nickel(I) and Palladium(I) Complexes Using Diphosphine Ligands with Large Bites

Alex Miedaner,[†] R. Curtis Haltiwanger,[‡] and Daniel L. DuBois*,[†]

Received April 6, 1990

Nickel and palladium complexes of the type $[M(L_2)_2](BF_4)_2$ and $[M(L_2)(L_2')](BF_4)_2$ (where L_2 and L_2' are diphosphine ligands) have been synthesized. The lowest energy electronic absorption band for the nickel complexes decreases in energy as the bite size of the diphosphine ligand increases. Similarly, the half-wave potentials for the Ni(II/I) and Pd(II/0) couples become more positive as the bite size increases. Structural studies of $[Ni(dppm)_2](BF_4)_2$ (where dppm is bis(diphenylphosphino)methane) and $[Ni(dppb)_2](PF_6)_2$ (where dppb is 1,2-bis(diphenylphosphino)benzene) show that increasing the bite size of the diphosphine ligands results in larger tetrahedral distortions. $[Ni(dppm)_2](BF_4)_2$ ($C_{50}H_{44}B_2F_8NiP_4$) crystallizes in the monoclinic space group $P2_1/n$ with a = 11.158 (10) Å, b = 17.43 (2) Å, c = 12.849 (11) Å, β = 111.38 (7)°, V = 3228 Å^3, and Z = 2. The structure was refined to R = 0.155 and R_w = 0.201 for 1005 independent reflections with $F_o > 6\sigma(F_o)$. $[Ni(dppb)_2](PF_6)_2$ ($C_{74}H_{64}F_{12}NiP_6$) crystallizes in space group $P\bar{1}$ with a = 11.359 (6) Å, b = 13.960 (5) Å, c = 21.297 (7) Å, α = 84.69 (3)°, β = 84.79 (4)°, γ = 78.96 (3)°, V = 3298 (2) Å^3, and Z = 2. The structure was refined to R = 0.072 and R_w = 0.085 for 2333 independent reflections with $F_o > 6\sigma(F_o)$. The tetrahedral distortion observed for $[Ni(dppb)_2](PF_6)_2$ was modeled by using extended Hückel calculations. These calculations indicate that the observed distortion may have an electronic as well as a steric component. The calculations also allow rationalization of the electronic absorption spectra, electrochemical data, and the stability of the Ni(I) and Pd(I) complexes $[Ni(dppp)_2](BF_4)$ (where dppp is 1,3-bis(diphenylphosphino)propane) and $[Pd(dppx)_2](BF_4)$ (where dppx is α,α'-bis(diphenylphosphino)-*o*-xylene). Complexes containing the ligand dppm have a marked tendency to become five-coordinate, as indicated by the structural determination of $[Ni(dppm)_2(CH_3CN)](PF_6)_2$. The latter complex ($C_{59}H_{55}F_{12}NNiP_6$) crystallizes in space group $P4/m$ with a = 19.363 (4) Å, c = 15.526 (4) Å, V = 5822 (2) Å^3, and Z = 4. The structure was refined to R = 0.048 and R_w = 0.062 for 3470 independent reflections with $F_o > 6\sigma(F_o)$.

Introduction

Nickel and palladium complexes catalyze the electrochemical reduction of CO_2,[1,2] the reductive coupling of aryl halides to biphenyls and binaphthyls,[3] and the reduction of alkyl halides.[4] These reactions are thought to involve Ni(I) or Pd(I) complexes as intermediates.[1-5] Dimerization of ethylene to butene appears to involve Pd(I) intermediates,[6] and a number of stoichiometric reactions involve Ni(I), Pd(I), or Pt(I) intermediates.[7,8] Although several mononuclear Ni(I) and Pd(I) complexes are known,[9,10] our understanding of the factors important in stabilizing these complexes to disproportionation is limited.

Electrochemical studies of nickel complexes containing monodentate phosphine ligands have shown that bond formation and cleavage reactions frequently precede or follow electron transfer.[11] These reactions complicate the assessment of the relative thermodynamic stabilities of different oxidation states. Their occurrence is the result of nickel preferring different coordination numbers and different types of ligands as the oxidation state changes. The coordination number of Ni(0) and Ni(I) phosphine complexes is normally 4, and the I/0 redox couple is reversible in most cases.[11] Nickel(II) complexes frequently have coordination

[†] Solar Energy Research Institute.
[‡] University of Colorado.

(1) Beley, M.; Collin, J. P.; Romain, R.; Sauvage, J. P. *J. Am. Chem. Soc.* **1986**, *108*, 7461.
(2) DuBois, D. L.; Miedaner, A. *J. Am. Chem. Soc.* **1987**, *109*, 113. DuBois, D. L.; Miedaner, A. Unpublished results.
(3) Semmelhack, M. F.; Helquist, P. M.; Jones, L. D.; Keller, L.; Mendelson, L.; Ryono, L. S.; Smith, J. G.; Stauffer, R. D. *J. Am. Chem. Soc.* **1981**, *103*, 6460. Semmelhack, M. F.; Helquist, P. M.; Jones, L. D. *J. Am. Chem. Soc.* **1971**, *93*, 5908. Troupel, M.; Rollin, Y.; Sibille, S.; Fauvarque, J. F.; Perichon, J. *J. Chem. Res., Synop.* **1980**, 26. Schiavon, G.; Bontempelli, G.; Corain, B. *J. Chem. Soc., Dalton Trans.* **1981**, 1074. Saraev, V. V.; Schmidt, F. K.; Larin, G. M.; Thach, V. S.; Lipovich, V. G. *Bull. Acad. Sci. USSR, Div. Chem. Sci.* (*Engl. Transl.*) **1974**, *23*, 2549.
(4) Stolzenberg, A. M.; Stershic, M. T. *J. Am. Chem. Soc.* **1988**, *110*, 5397.
(5) Amatore, C.; Jutand, A. *Organometallics* **1988**, *7*, 2203. Colon, I.; Kelsey, D. R. *J. Org. Chem.* **1986**, *51*, 2627. Tsou, T. T.; Kochi, J. K. *J. Am. Chem. Soc.* **1979**, *101*, 6319; **1979**, *101*, 7547.
(6) Ghosh, A. K.; Kevan, L. *J. Am. Chem. Soc.* **1988**, *110*, 8044.
(7) Kamer, A. V.; Osborn, J. A. *J. Am. Chem. Soc.* **1974**, *96*, 7832. Stille, J. K.; Lau, K. *Acc. Chem. Res.* **1977**, *10*, 434. Lappert, M. F.; Lendor, P. W. *Adv. Organomet. Chem.* **1976**, *14*, 345.
(8) Ram, M. S.; Bakac, A.; Espenson, J. H. *Inorg. Chem.* **1988**, *27*, 4231; **1988**, *27*, 2011. Bernhardt, P. V.; Lawrence, G. A.; Sauster, D. F. *Inorg. Chem.* **1988**, *27*, 4055.

0020-1669/91/1330-0417$02.50/0

Table I. Summary of Crystal and Refinement Data for Complexes

	$[Ni(dppm)_2](BF_4)_2$	$[Ni(dppb)_2](PF_6)_2$	$[Ni(dppm)_2(CH_3CN)](PF_6)_2$
empirical formula	$C_{50}H_{44}B_2F_8P_4Ni$	$C_{74}H_{64}F_{12}P_6Ni$	$C_{59}H_{55}F_{12}P_6NNi$
space group	monoclinic, $P2_1/n$	triclinic, $P\bar{1}$	tetragonal, $P4/m$
unit cell dimens			
a, Å	11.158 (10)	11.359 (6)	19.363 (4)
b, Å	17.43 (2)	13.960 (5)	
c, Å	12.849 (11)	21.297 (7)	15.526
α, deg		84.69 (3)	
β, deg	111.38 (7)	84.79 (4)	
γ, deg		78.96 (3)	
V, Å^3	3228 (4)	3298 (2)	5822 (2)
M_r	1001.1	1425.9	1250.6
Z	2	2	4
D(calc), g cm^{-3}	1.428	1.44	1.427
radiation (λ, Å)	Mo Kα (0.710 73)	Mo Kα (0.710 73)	Mo Kα (0.710 73)
T, °C	−80	22–24	22–24
μ, cm^{-1}	6.18	5.13	5.71
transm coeff	none applied	none applied	0.8713–0.9098
final R, R_w	15.5, 20.1	7.2, 8.5	4.8, 6.2

numbers of 5 or 6, for example $[Ni\{P(OMe)_3\}_5]^{2+}$ and $[Ni(CH_3CN)_4(PPh_3)_2]^{2+}$. They also frequently have hard anionic ligands such as halide ions, which do not bind well to nickel in the I or 0 oxidation states. For these reasons reversible II/I couples are not observed for $[Ni(CH_3CN)_4(PPh_3)_2]^{2+}$, $[Ni\{P(OMe_3)_3\}_5]^{2+}$, or $Ni(PPh_3)_2Br_2$.[11] However, for ligands with the proper combination of steric and electronic requirements such as PEt_3 and PEt_2Ph, four-coordinate Ni(II) complexes are formed that have reversible or quasi-reversible electron-transfer reactions for both the II/I and I/0 couples.[11] The observation of two reversible one-electron reductions allows the assessment of the stability of the +1 oxidation state to disproportionation.

By use of bidentate ligands with soft donor atoms, bond cleavage and formation reactions can be avoided. For example, the nickel complexes $[Ni(dppe)_2]^{2+}$ and $[Ni(Ph_2PCH_2CH_2SC_2H_5)_2]^{2+}$ both exhibit two reversible one-electron reductions, and $[Pd(dppe)_2]^{2+}$ and $[Pt(dppe)_2]^{2+}$ exhibit reversible two-electron reductions.[12] The Pd(I) and Pt(I) complexes are not observed, since they are unstable with respect to disproportionation to the II and 0 oxidation states. In this paper it is shown for $[M(diphos)_2]^{2+}$ complexes of nickel and palladium that increasing the bite size of the diphosphine ligand results in an increasingly large distortion of the complexes from a planar toward a tetrahedral geometry. This distortion results in the stabilization of the +1 oxidation state with respect to disproportionation.

Experimental Section

Physical Measurements. Infrared spectra were obtained on Nujol mulls with a Perkin-Elmer 599B spectrophotometer. All of the BF_4 salts show a strong infrared absorption between 900 and 1150 cm^{-1}. A Varian E109 spectrometer was used for obtaining EPR spectra. EPR spectra were recorded on dichloromethane solutions containing Ni(I) or Pd(I) complexes at concentrations of $\sim 1 \times 10^{-3}$ M. A JEOL FX90Q FT NMR spectrometer equipped with a tunable, variable-temperature probe was used to collect ^1H and ^{31}P NMR spectra. Chemical shifts for ^1H NMR spectra were referenced to Me_4Si by using deuterated solvent peaks as secondary reference signals. A capillary filled with phosphoric acid was used as an external reference for ^{31}P NMR spectra. All ^{31}P NMR spectra were proton decoupled. ^{31}P spectral simulations were performed by using the RACCOON program.[13]

Electrochemical measurements were carried out with a Cypress System computer-aided electrolysis system or a Princeton Applied Research Model 173 potentiostat equipped with a digital coulometer and a Model 175 universal programmer. A silver wire that had been dipped in concentrated nitric acid and then concentrated hydrochloric acid, rinsed with distilled water, and dried was used as a pseudoreference electrode. Ferrocene was used as an internal standard, and all potentials are reported vs the ferrocene/ferrocenium couple. For cyclic voltammetry, a glassy-carbon disk electrode obtained from Bioanalytical Systems, Inc., was used as a working electrode, and a platinum wire was used as a counter electrode. All compounds were studied by cyclic voltammetry over a range of scan rates from 50 to 500 mV/s. Working electrodes used for bulk electrolysis experiments were constructed from reticulated vitreous carbon obtained from the Electrosynthesis Co., Inc.

X-ray crystallographic measurements were carried out on a Siemens P3F autodiffractometer. Mo Kα radiation, monochromatized by diffraction off of a highly oriented graphite crystal, was used for all three studies. Crystals used for room-temperature studies were mounted and coated with epoxy. The crystal used in the low-temperature study was mounted and coated with Apiezon T grease. The crystals of $[Ni(dppm)_2](BF_4)_2$ were of low quality, but repeated attempts to obtain higher quality crystals were unsuccessful. Programs in the Siemens X-ray package were used for data collection and for structure solution and refinement. Details of the experimental conditions are given in the supplementary material. Table I summarizes the crystal data and structure refinement details. Table II lists selected atomic coordinates and equivalent isotropic displacement factors for $[Ni(dppm)_2](BF_4)_2$, $[Ni(dppb)_2](PF_6)_2$, and $[Ni(dppm)_2(CH_3CN)](PF_6)_2$, respectively.

Materials. Acetonitrile and dichloromethane were dried by distillation from calcium hydride under nitrogen. Toluene, tetrahydrofuran (THF), and hexanes were distilled from sodium benzophenone ketyl under nitrogen. Anhydrous ethanol was used as obtained from Aldrich Chemical Co. Nitromethane (99+% and 96%) and nitromethane-d_3 were purchased from Aldrich Chemical Co. During the course of our investigation we observed that the ^{31}P NMR spectra and electronic absorption spectra of $[Ni(dppm)_2](BF_4)_2$ were different in nitromethane and nitromethane-d_3. This phenomenon was not observed for any of the other complexes that we investigated. Addition of acetonitrile to solutions of nitromethane-d_3 produced spectra identical with those observed in proteonitromethane. Attempts to purify the nitromethane by distillation from P_2O_5 and more elaborate procedures were unsuccessful.[14] Consequently, nitromethane-d_3 was used in all studies of $[Ni(dppm)_2](BF_4)_2$ with the exception of recrystallization. The ligands bis(diphenylphosphino)methane (dppm), bis(diphenylphosphino)ethane (dppe), *cis*-1,2-bis(diphenylphosphino)ethylene (dppv), 1,2-bis(diphenylphosphino)-benzene (dppb), 1,3-bis(diphenylphosphino)propane (dppp), and α,α'-bis(diphenylphosphino)-*o*-xylene (dppx) were purchased from Strem

(9) Sacconi, L.; Ghilardi, C. A.; Mealli, C.; Zanobini, F. *Inorg. Chem.* **1975**, *14*, 1380. Gleizes, A.; Dartiguenave, M.; Dartiguenave, Y.; Galy, J.; Klein, H. F. *J. Am. Chem. Soc.* **1977**, *99*, 5187. Aresta, M.; Nobile, C. F.; Sacco, A. *Inorg. Chim. Acta* **1975**, *12*, 167. Porri, L.; Ghallazzi, M. C.; Vitulli, G. *J. Chem. Soc., Chem. Commun.* **1967**, 228. Sacconi, L.; Midollini, S. *J. Chem. Soc., Dalton Trans.* **1972**, 1213. Sacconi, L.; Dapporto, P.; Stoppioni, P. *Inorg. Chem.* **1976**, *15*, 325. DuBois, D. L.; Miedaner, A. *Inorg. Chem.* **1986**, *25*, 4642. Cecconi, F.; Midollini, S.; Orlandini, A. *J. Chem. Soc., Dalton Trans.* **1983**, 2263.
(10) Broadley, K.; Lane, G. A.; Connelly, N. G.; Geiger, W. E. *J. Am. Chem. Soc.* **1983**, *105*, 2486. Lane, G. A.; Geiger, W. E.; Connelly, N. G. *J. Am. Chem. Soc.* **1987**, *109*, 402.
(11) Bontempelli, G.; Magno, F.; Corain, B.; Schiavon, G. *J. Electroanal. Chem. Interfacial Electrochem.* **1979**, *103*, 243. Bontempelli, G.; Magno, F.; Schiavon, G.; Corain, B. *Inorg. Chem.* **1981**, *20*, 2579. Jasinski, R. *J. Electrochem. Soc.* **1983**, *130*, 834.
(12) Martelli, M.; Pilloni, G.; Zotti, G.; Daolio, S. *Inorg. Chim. Acta* **1974**, *11*, 155. Zotti, G.; Pilloni, G.; Rigo, P.; Martelli, M. *J. Electroanal. Chem. Interfacial Electrochem.* **1981**, *124*, 277.
(13) Schatz, P. F. Project SERAPHIM, National Science Foundation, Science Education.
(14) Hathaway, B. J.; Holah, D. G.; Underhill, A. E. *J. Chem. Soc.* **1962**, 2444.

Table II. Selected Atomic Coordinates ($\times 10^4$) and Equivalent Isotropic Displacement Parameters ($Å^2 \times 10^3$)

	x/a	y/b	z/c	U(eq)[a]
		$[Ni(dppm)_2](BF_4)_2$		
Ni(1)	0	0	0	28 (2)*
P(1)	−1899 (7)	572 (6)	−746 (6)	30 (3)*
P(2)	37 (7)	659 (6)	−1474 (6)	28 (3)*
C(1)	−1252 (27)	1278 (19)	−1442 (26)	36 (9)
C(11)	−3052 (17)	8 (12)	−1827 (16)	39 (8)
C(21)	−2752 (18)	1025 (9)	15 (16)	30 (8)
C(31)	−554 (18)	164 (9)	−2775 (16)	19 (7)
C(41)	1397 (19)	1210 (10)	−1492 (17)	31 (8)
		$[Ni(dppb)_2](PF_6)_2$		
Ni(1)	2834 (2)	8744 (2)	2559 (1)	34 (1)*
P(1)	1328 (4)	9702 (3)	3044 (2)	38 (2)*
P(2)	1986 (5)	7518 (3)	2984 (2)	43 (2)*
P(3)	4629 (4)	7901 (3)	2306 (2)	39 (2)*
P(4)	3373 (5)	9951 (3)	1913 (2)	42 (2)*
C(11)	734 (10)	8953 (8)	3670 (5)	39 (5)
C(12)	1010	7941	3638	43 (5)
C(13)	551	7323	4102	55 (6)
C(14)	−184	7718	4597	60 (6)
C(15)	−459	8730	4629	65 (6)
C(16)	0	9348	4166	55 (6)
C(21)	5183 (10)	8474 (8)	1588 (4)	40 (5)
C(22)	4658	9451	1440	47 (5)
C(23)	5125	9991	934	59 (6)
C(24)	6118	9553	578	62 (6)
C(25)	6642	8576	726	61 (6)
C(26)	6175	8036	1232	59 (6)
C(31)	1 (9)	10226 (8)	2615 (5)	52 (6)
C(41)	1807 (10)	10635 (8)	3446 (5)	43 (5)
C(51)	2767 (10)	6328 (6)	3279 (5)	43 (5)
C(61)	1024 (10)	7306 (8)	2389 (5)	38 (5)
C(71)	5523 (10)	8183 (7)	2911 (5)	41 (5)
C(81)	5069 (10)	6603 (6)	2235 (6)	40 (5)
C(91)	2236 (9)	10464 (8)	1359 (5)	40 (5)
C(101)	3908 (9)	10945 (7)	2220 (5)	37 (5)
		$[Ni(dppm)_2(CH_3CN)](PF_6)_2$		
Ni(1)	7577 (1)	2288 (1)	0	38 (1)*
N(1)	7162 (2)	1288 (3)	0	51 (1)
C(3)	7181 (3)	702 (3)	0	49 (2)*
C(4)	7233 (5)	−59 (3)	0	91 (3)*
P(1)	6756 (1)	2702 (1)	856 (1)	44 (1)*
P(2)	8477 (1)	2123 (1)	855 (1)	41 (1)*
C(1)	6107 (3)	2642 (3)	0	52 (2)*
C(2)	9089 (3)	2182 (3)	0	43 (2)*
C(11)	6470 (2)	2236 (2)	1799 (3)	50 (1)*
C(21)	8515 (2)	1261 (2)	1318 (3)	43 (1)*
C(31)	6787 (2)	3604 (2)	1168 (3)	57 (2)
C(41)	8722 (2)	2719 (2)	1700 (3)	46 (1)*

[a] For U(eq) values marked with asterisks, the equivalent isotropic U is defined as one-third of the trace of the orthogonalized U_{ij} tensor.

Chemicals, Inc. The metal complexes $[Ni(CH_3CN)_6](BF_4)_2 \cdot {}^1/_2CH_3CN$,[15] $[Pd(CH_3CN)_4](BF_4)_2$,[16] $[Ni(dppe)_2]$, $[Ni(dppp)_2]$, and $[Ni(dppb)_2]$[17] were prepared by literature methods.

Syntheses. Representative preparations of Ni(II) and Pd(II) complexes are given below. Similar methods were used to prepare other complexes described in this paper. All reactions were carried out by using standard Schlenk techniques. The complexes give satisfactory elemental analyses. The elemental analyses were performed by either Spang Microanalytical Laboratories or Huffman Laboratories, Inc.

$[Ni(dppm)_2](BF_4)_2$. A blue solution of $[Ni(CH_3CN)_6](BF_4)_2 \cdot {}^1/_2CH_3CN$ (1.5 g, 3 mmol) in acetonitrile (30 mL) was added to a stirred solution of dppm (2.30 g, 6 mmol) in dichloromethane (50 mL). The resulting dark red solution was stirred for 1 h at room temperature, and then the volume of the solution was reduced to ca. 50 mL in vacuo. Addition of ethanol produced a yellow precipitate, which was collected by filtration and dried in vacuo at 80 °C for 3 h. The yield was 2.50 g (83%). Anal. Calcd for $C_{50}H_{44}B_2F_8NiP_4$: C, 59.98; H, 4.44; P, 12.37. Found: C, 60.11; H, 4.59; P, 12.68. Crystals of $[Ni(dppm)_2](BF_4)_2$ may be obtained by dissolving the product in hot nitromethane and slowly cooling the solution to room temperature. Crystallization of the product from a mixture of acetonitrile and toluene at −20 °C yields crystals of $[Ni(dppm)_2(CH_3CN)](BF_4)_2$. Similar results are obtained by using PF_6^- anions instead of BF_4^- anions.

$[Ni(dppp)(dppm)](BF_4)_2$. Acetonitrile (30 mL) was added to a mixture of $[Ni(CH_3CN)_6](BF_4)_2 \cdot {}^1/_2CH_3CN$ (0.50 g, 1.0 mmol), dppp (0.41 g, 1.0 mmol), and dppm (0.38 g, 1.0 mmol). The resulting red-orange solution was stirred for 2 h at room temperature. The solvent was removed in vacuo to produce a yellow solid, which was recrystallized from hot nitromethane. The yield was 0.76 g (79%). Anal. Calcd for $C_{52}H_{48}B_2F_8NiP_4$: C, 60.68; H, 4.71. Found: C, 60.08; H, 4.91.

$[Ni(dppb)(dppp)](BF_4)_2$. An acetonitrile solution (30 mL) containing $[Ni(CH_3CN)_6](BF_4)_2 \cdot {}^1/_2CH_3CN$ (0.50 g, 1.0 mmol) was added to a dichloromethane solution (30 mL) containing dppp (0.41 g, 1.0 mmol). The resulting solution was stirred for 30 min. Solid dppb (0.45 g, 1.0 mmol) was added and the reaction mixture stirred for 1 h. A yellow solid was isolated by removing the solvent in vacuo. Recrystallization from a mixture of nitromethane and diethyl ether yielded 0.62 g (57%). The product at this point was an approximately 20:1 mixture of $[Ni(dppb)(dppp)](BF_4)_2$ and $[Ni(dppb)_2](BF_4)_2$, as indicated by ^{31}P NMR spectroscopy and cyclic voltammetry. Further efforts at purification did not improve the purity of the product.

$[Ni^I(dppp)_2](BF_4)$. Acetonitrile (50 mL) was added to a mixture of $[Ni(CH_3CN)_6](BF_4) \cdot {}^1/_2CH_3CN$ (0.50 g, 1.0 mmol) and dppp (0.83 g, 2.0 mmol). The resulting reaction mixture was stirred to produce a red solution, which was added to a suspension of $[Ni^0(dppp)_2]$ (0.88 g, 1.0 mmol) in acetonitrile (50 mL). The reaction mixture was stirred overnight and the resulting yellow solution concentrated to 20 mL to produce a yellow precipitate. The product was collected by filtration and recrystallized from a mixture of dichloromethane and hexanes to yield 1.50 g (77%). No EPR spectrum was observed for the product. Magnetic susceptibility measurements gave $\chi_g = 1.54 \times 10^{-6}$ and $\mu_{eff} = 2.10\ \mu_B$. Anal. Calcd for $C_{54}H_{52}BF_4NiP_4$: C, 66.83; H, 5.41; Ni, 6.05; P, 12.77. Found: C, 66.48; H, 5.26; Ni, 6.06; P, 12.62.

$[Pd^{II}(dppp)_2](BF_4)_2$. A solution of dppp (0.83 g, 2.0 mmol) in dichloromethane (30 mL) was added to a stirred solution of $[Pd(CH_3CN)_4](BF_4)_2$ (0.45 g, 1.0 mmol) in acetonitrile (30 mL) to produce a white precipitate. The reaction mixture was stirred for 2 h, and the precipitate was collected by filtration. After the solid was dried at 50 °C for 3 h in vacuo, the yield was 0.86 g (78%). Anal. Calcd for $C_{54}H_{52}B_2F_8P_4Pd$: C, 58.69; H, 4.75; P, 11.21; Pd, 9.63. Found: C, 58.38; H, 4.73; P, 11.01; Pd, 9.44.

$[Pd^{II}(dppp)(CH_3CN)_2](BF_4)_2$. A solution of dppp (0.41 g, 1.0 mmol) in dichloromethane (30 mL) was added to a stirred solution of $[Pd(CH_3CN)_4](BF_4)_2$ (0.45 g, 1.0 mmol) in acetonitrile (30 mL). The resulting yellow solution was stirred for 1 h and the solvent removed on a vacuum line at 60 °C to produce a yellow solid. Anal. Calcd for $C_{31}H_{32}B_2F_8N_2P_2Pd$: C, 48.07; H, 4.17; N, 3.62; P, 8.00; Pd, 13.74. Found: C, 47.37; H, 4.28; N, 3.56; P, 7.47; Pd, 13.21.

$[Pd^{II}(dppp)(PEt_3)_2](BF_4)_2$. Triethylphosphine (0.30 mL, 2.0 mmol) was added via syringe to a solution of $[Pd(dppp)(CH_3CN)_2](BF_4)_2$ (0.77 g, 1.0 mmol) in dichloromethane (50 mL). The resulting mixture was stirred for 2 h and the solvent removed in vacuo. Recrystallization of the crude product from a mixture of dichloromethane and hexanes yielded 0.52 g (56%) of a white solid. Anal. Calcd for $C_{39}H_{56}B_2F_8P_4Pd$: C, 50.43; H, 6.09; P, 13.34; Pd, 11.46. Found: C, 50.31; H, 5.93; P, 13.11; Pd, 11.29.

$[Pd(dppx)(dppm)](BF_4)_2$. A solution of dppx (0.47 g, 1.0 mmol) in dichloromethane (20 mL) was added to a solution of $[Pd(CH_3CN)_4](BF_4)_2$ in acetonitrile (20 mL). The resulting solution was stirred for 15 min, and then a solution of dppm (0.38 g, 1.0 mmol) in 20 mL of dichloromethane was added. The reaction mixture was stirred for 2 h and the solvent removed with a vacuum line. The crude product was recrystallized from a mixture of dichloromethane and diethyl ether. The resulting yellow powder was collected on a frit by filtration and dried for 3 h at 50 °C in vacuo with a yield of 0.85 g (74%). Anal. Calcd for $C_{57}H_{50}B_2F_8P_4Pd$: C, 60.10; H, 4.43; P, 10.88; Pd, 9.34. Found: C, 59.80; H, 4.58; P, 10.70; Pd, 9.16.

Results

Synthesis and Characterization of Metal Complexes. The preparations of the $[M(diphos)_2](BF_4)_2$ (diphos = diphosphine) complexes from $[Ni(CH_3CN)_6](BF_4)_2$ and $[Pd(CH_3CN)_4](BF_4)_2$ and the appropriate diphosphine ligands are straightforward with the exception that $[Ni(dppp)_2](BF_4)_2$ could not be obtained

(15) Sen, A.; Ta-Wang, L. *J. Am. Chem. Soc.* **1981**, *103*, 4627.
(16) Ittel, S. D. In *Inorganic Synthesis*; MacDiarmid, A. G., Ed.; McGraw-Hill: New York, 1977; Vol. 17, p 117.
(17) Gordon, A. J.; Ford, R. A. *The Chemist's Companion*; Wiley: New York, 1972; p 436. Fieser, L. F.; Fieser, M. *Reagents for Organic Synthesis*; Wiley: New York, 1967; Vol. 1, p 739.

Table III. ^{31}P NMR and Electronic Absorption Data for $[M(L_2)_2](BF_4)_2$ and $[M(L_A)_2(L_X)_2](BF_4)_2$[a] Complexes

	NMR data				abs data	
compd	δ_A (δ_X)	$J_{AA'}$ ($J_{XX'}$)	J_{AX} ($J_{AX'}$)	solv	λ_{max}[b]	solv
$[Ni(dppm)_2](BF_4)_2$	−26.7			CD_3NO_2	<400	CD_3NO_2
$[Ni(dppm)_2(CH_3CN)](BF_4)_2$	−35.4			CD_3CN	436	CH_3CN
$[Ni(dppe)_2](BF_4)_2$	55.2			CD_3CN	412 (sh)	CH_2Cl_2
	54.7			CD_3NO_2	410 (sh)	CH_3CN
$[Ni(dppv)_2](BF_4)_2$	65.8			CD_3CN	438	CH_3NO_2
	67.4			CD_3NO_2	440	CH_3CN
$[Ni(dppb)_2](BF_4)_2$	56.9			CD_3CN	434	CH_3NO_2
	57.4			CD_3NO_2	432	CH_3CN
$[Ni(dppp)_2](BF_4)_2$	−7.8			CD_2Cl_2	510	CH_2Cl_2
$[Ni(dppe)(dppm)](BF_4)_2$	57.41	−33.9	−47.0	CD_3NO_2	412 (sh)	CH_3NO_2
	(−24.5)	(−90.1)	(193.5)		434 (sh)	CH_3CN
$[Ni(dppp)(dppm)](BF_4)_2$	−2.44	−78.45	−62.2	CD_2Cl_2	414	CH_2Cl_2
	(−23.76)	(−86.95)	(191.8)		458	CH_3CN
$[Ni(dppb)(dppp)](BF_4)_2$	52.52	−37.2	−55.6	CD_2Cl_2	442	CH_2Cl_2
	(−4.40)	(−77.1)	(175.8)		442	CH_3CN
$[Pd(dppm)_2](BF_4)_2$	−32.5			DMSO		
$[Pd(dppe)_2](BF_4)_2$	57.1			DMSO		
$[Pd(dppb)_2](BF_4)_2$	52.6			DMSO		
$[Pd(dppp)_2](BF_4)_2$	0.0			DMSO		
$[Pd(dppx)_2](BF_4)_2$	6.4			CD_2Cl_2		
$[Pd(dppp)(CH_3CN)_2](BF_4)_2$	10.9			CD_2Cl_2		
$[Pd(dppx)(dppm)](BF_4)_2$	3.12	−19.6	−16.8	CD_2Cl_2		
	(−29.92)	(−59.5)	(352.0)			
$[Pd(PEt_3)_2(dppp)](BF_4)_2$	14.66	−31.4	−19.4	CD_3NO_2		
	(−0.4)	(−51.3)	(338.4)			
$[Pd(PEt_3)(dppp)]_2(BF_4)_2$	21.7_A	416.3 (J_{AB})		CD_2Cl_2		
	1.0_B	−12.3 (J_{AX})				
	13.1_X	−39.1 (J_{BX})				

[a] For all complexes the ligand corresponding to chemical shift δ_A is given first and the ligand corresponding to chemical shift δ_X is given in parentheses. All chemical shifts are referenced to external H_3PO_4. All J values are given in Hz. [b] λ_{max} is given in nanometers, and sh represents a shoulder with no well-defined peak.

analytically pure. Structures **1**–**6** define the various ligands discussed in this paper.

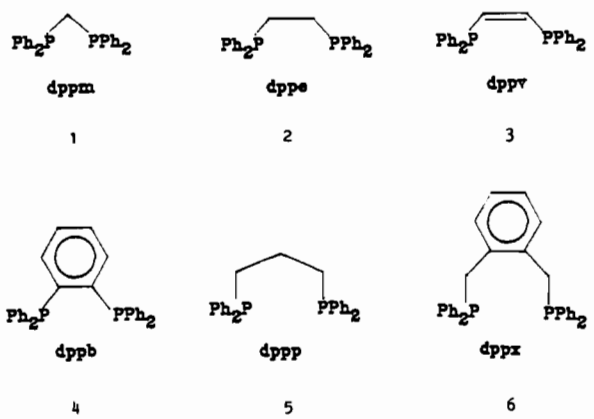

The preparations of mixed-ligand complexes of the type $[M(L_2)(L_2')](BF_4)_2$ are given in detail in the Experimental Section, since the results obtained depend somewhat on the nature of the diphosphine ligands. Mixing solutions of $[Ni(dppm)_2](BF_4)_2$ and $[Ni(dppe)_2](BF_4)_2$ resulted in an equilibrium between $[Ni(dppe)(dppm)](BF_4)_2$ and the reactants, as determined by ^{31}P NMR spectroscopy. The equilibrium concentrations of the reactants are estimated to be approximately 10% of the concentration of the product. Similarly, the reaction of $[Ni(CH_3CN)_6](BF_4)_2$ with 1 equiv each of dppb and dppp resulted in a mixture of $[Ni(dppp)(dppb)](BF_4)_2$ and $[Ni(dppb)_2](BF_4)_2$ in an approximately 20:1 ratio, which we were unable to purify further. In contrast, reaction of $[Ni(CH_3CN)_6](BF_4)_2$ with 1 equiv each of dppm and dppp resulted in the formation of $[Ni(dppp)(dppm)](BF_4)_2$, which can be isolated in pure form. Reaction of 1 equiv of dppp or dppx with $[Pd(CH_3CN)_4](BF_4)_2$ results in the clean formation of $[Pd(dppp)(CH_3CN)_2](BF_4)_2$ or $[Pd(dppx)(CH_3CN)_2](BF_4)_2$, respectively. These complexes are similar to [Pd(dppe)(dimethyl sulfoxide)]$^{2+}$ described recently.[18] Addition of a second bidentate ligand or monodentate ligands to these complexes allows easy preparation of mixed-ligand complexes such as $[Pd(dppp)(PEt_3)_2](BF_4)_2$ and $[Pd(dppx)(dppm)](BF_4)_2$, as shown in eq 1.

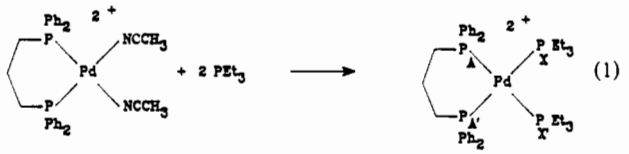

(1)

7 8

The Ni(II) and Pd(II) complexes have been characterized by elemental analyses and/or X-ray structure determinations,[31]P and ^1H NMR spectroscopy, cyclic voltammetry, and electronic absorption spectroscopy. The ^{31}P NMR spectra of the $[M(diphos)_2](BF_4)_2$ complexes (Table III) consist of single resonances with chemical shifts appropriate for phosphorus in four-, five-, six-, and seven-membered rings.[19] The mixed-ligand complexes $[M(L_2)(L_2')](BF_4)_2$ have AA'BB' or AA'XX' spin systems (see structure **8** for labeling) and consequently exhibit second-order spectra. These spectra can be simulated with the parameters listed in Table III. The assignments of chemical shifts for the bidentate ligands are based on their similarity to the chemical shifts observed for the analogous $[M(diphos)_2](BF_4)_2$ complexes. The largest coupling constant between the A_2 and X_2 spin systems is assigned to the trans coupling constant, $J_{AX'}$, with the smaller value attributed to the cis interligand coupling constant, J_{AX}. The values of the intraligand coupling constants are given by $J_{AA'}$ and $J_{XX'}$. These values may be interchanged without affecting the appearance of the spectrum, and the assignments have been made on the basis of their similarity to other complexes with similar

(18) Hartley, F. R.; Murray, S. G.; Wilkinson, A. *Inorg. Chem.* **1989**, *28*, 549.
(19) Garrou, P. E. *Chem. Rev.* **1981**, *81*, 229.

Table IV. Summary of Cyclic Voltammetry and EPR Data for $[M(L_2)_2](BF_4)_2$ and $[M(L_A)_2(L_X)_2](BF_4)_2$ Complexes[a]

compd	$E_{1/2}$(II/I)[b]	$E_{1/2}$(II/0)[b]	$E_{1/2}$(I/0)[b]	solv	g	A[c]
$[Ni(dppm)_2](BF_4)_2$	−0.70 (140)		−0.96 (62)	CD_3NO_2		
$[Ni(dppm)_2(CH_3CN)](BF_4)_2$	−0.77 (93)		−1.05 (127)	CH_3CN		
$[Ni(dppe)_2](BF_4)_2$	−0.66 (80)		−0.95 (65)	CH_2Cl_2	2.07	60
	−0.71 (65)		−0.89 (60)	CH_3CN		
$[Ni(dppb)_2](BF_4)_2$	−0.54 (75)		−0.98 (70)	CH_2Cl_2	2.07	65
	−0.48 (60)		−0.79 (62)	CH_3CN		
$[Ni(dppv)_2](BF_4)_2$	−0.48 (67)		−0.91 (62)	CH_2Cl_2	2.06	62
	−0.52 (65)		−0.83 (67)	CH_3CN		
$[Ni(dppp)_2](BF_4)$	−0.12 (90)		−0.95 (75)	CH_2Cl_2		
	−0.19 (E_{pa}, irr)		−0.91 (60)	CH_3CN		
$[Ni(dppe)(dppm)](BF_4)_2$	−0.72 (72)		−1.00 (69)	CH_2Cl_2	2.08	65
	−0.76 (67)		−0.96 (63)	CH_3CN		
$[Ni(dppp)(dppm)](BF_4)_2$	−0.69 (102)		−1.04 (88)	CH_2Cl_2	2.10	
	−0.63 (71)		−0.99 (60)	CH_3CN		
$[Ni(dppb)(dppp)](BF_4)_2$	−0.40 (85)		−0.95 (83)	CH_2Cl_2		
	−0.39 (63)		−0.86 (62)	CH_3CN		
$[Pd(dppm)_2](BF_4)_2$		−1.04 (E_{pc}, irr)		DMSO		
		−0.71 (E_{pa}, irr)				
$[Pd(dppe)_2](BF_4)_2$		−1.04 (35)		DMSO		
$[Pd(dppb)_2](BF_4)_2$		−0.99 (35)		CH_3CN		
$[Pd(dppp)_2](BF_4)_2$		−0.85 (35)		DMSO		
$[Pd(dppx)_2](BF_4)_2$	−0.51 (60)		−0.63 (62)	CH_2Cl_2		
$[Pd(dppx)(dppm)](BF_4)_2$		−0.87 (45)		CH_3CN		
$[Pd(PEt_3)_2(dppp)](BF_4)_2$	−0.89 (E_{pc}, irr)			CH_3CN		

[a] All potentials are in volts and are referenced to the ferrocene/ferrocenium couple. [b] Numbers in parentheses indicate the peak to peak separation of the waves in mV for scan rates of 50 or 100 mV/s. [c] The hyperfine coupling constants are in gauss.

ligands.[19] The chemical shifts of $[Ni(dppm)_2](BF_4)_2$ in acetonitrile and nitromethane-d_3 differ by 9 ppm. This difference in chemical shift values is attributed to coordination of acetonitrile by the cation $[Ni(dppm)_2]^{2+}$ to form $[Ni(dppm)_2(CH_3CN)]^{2+}$, as verified by structural studies described below. Addition of acetonitrile to solutions of $[Ni(dppm)(dppp)](BF_4)_2$ and $[Ni(dppm)(dppe)](BF_4)_2$ results in a broadening of these resonances. This broadening is attributed to an equilibrium between four- and five-coordinate complexes arising from coordination of acetonitrile.

The nickel(II) compounds exhibit an electronic absorption between 400 and 550 nm, as shown in Table III. This band is assigned to a transition from an a_{1g} orbital to a b_{1g} orbital of these square-planar complexes.[20] It can be seen from the data in Table III that increasing the bite size of the chelating diphosphine ligands results in a decrease in the transition energy of this low-energy band in noncoordinating solvents such as dichloromethane or nitromethane. This transition occurs at higher energies for the palladium complexes and is obscured by charge-transfer bands that are observed between 200 and 400 nm for both the palladium and nickel complexes. For $[Ni(dppm)_2](BF_4)_2$, $[Ni(dppm)(dppe)](BF_4)_2$, and $[Ni(dppm)(dppp)](BF_4)_2$ a red shift of the lowest energy band is observed in acetonitrile consistent with increasing the energy of the a_{1g} (dz^2) orbital upon coordination of acetonitrile. The remaining complexes do not exhibit significant red shifts in acetonitrile.

As discussed above, we were unable to isolate an analytically pure sample of $[Ni(dppp)_2](BF_4)_2$. However, the Ni(I) complex, $[Ni(dppp)_2](BF_4)$, can be prepared by the comproportionation of $[Ni(CH_3CN)_6](BF_4)_2$ and $[Ni(dppp)_2]$ in the presence of 2 equiv of dppp. The isolated Ni(I) complex exhibited no EPR spectrum in the solid state or in solution at room temperature. Magnetic susceptibility measurements of the solid gave an effective magnetic moment of 2.10 μ_B for this complex. This value is in the range observed for other tetrahedral d^9 complexes (1.93–2.40 μ_B).[9,21] The failure to observe a solution EPR spectrum is attributed to fast relaxation of the unpaired electron in a distorted tetrahedral geometry. The ^{31}P NMR and electronic absorption spectra reported for $[Ni(dppp)_2](BF_4)_2$ were obtained on dichloromethane solutions generated by a controlled-potential electrolysis of $[Ni(dppp)_2](BF_4)$. Cyclic voltammograms recorded before and after electrolysis were identical, which indicates that $[Ni(dppp)_2](BF_4)_2$ is stable in this solvent.

Electrochemical Studies. The nickel complexes described above undergo two reversible or quasi-reversible one-electron reductions in at least one solvent, as shown in Table IV. The reversibility of the couples is indicated by the approximately 60-mV peak to peak separation observed for both redox waves in acetonitrile at sweep rates of 50–100 mV/s and an i_{pc}/i_{pa} ratio close to 1.0. At higher sweep rates of 0.4–10 V/s the Ni(II/I) couple becomes quasi-reversible with the wave corresponding to this couple exhibiting larger peak to peak separations than observed for the waves assigned to the Ni(I/0) couple and the ferrocene/ferrocenium couple. This indicates that electron transfer for the Ni(II/I) couple is slower than for the Ni(I/0) couple. In dichloromethane or nitromethane the same two reduction waves are observed, but the peak to peak separations, ΔE_p, are somewhat larger due to uncompensated resistance. In all cases except $[Ni(dppm)_2(CH_3CN)](BF_4)_2$, ΔE_p for the Ni(I/0) couple is within 5 mV of the ferrocene/ferrocenium couple; therefore, the difference between ΔE_p for the II/I couple and ΔE_p for the I/0 couple provides an estimation of the contribution to ΔE_p arising from slow electron transfer. Controlled-potential electrolysis of the Ni(II) complexes at potentials between the two waves resulted in the passage of 1.0 ± 0.1 Faradays of charge/mol of complex. Dichloromethane solutions of the resulting Ni(I) complexes were characterized by EPR spectroscopy. The EPR spectra generally exhibit five-line patterns attributed to the hyperfine coupling of the four phosphorus atoms with nuclear spins of $^1/_2$. The observed g and A values are shown in Table IV and are consistent with other Ni(I) complexes.[22] For $[Ni(dppm)_2](BF_4)_2$ attempts to characterize the product(s) formed on reduction (1.1 Faradays/mol of complex) were unsuccessful. No EPR signals were observed for dichloromethane solutions, and ^{31}P NMR spectra showed only residual starting material.

The spectral data indicating the existence of four-coordinate $[Ni(dppm)_2](BF_4)_2$ and five-coordinate $[Ni(dppm)_2(CH_3CN)](BF_4)_2$ described above led us to examine the effect of adding acetonitrile to solutions of Ni(II) complexes in a noncoordinating solvent such as dichloromethane or nitromethane. With the exception of $[Ni(dppm)_2](BF_4)_2$, concentrations of

(20) Figgis, B. N. *Introduction to Ligand Fields*; Interscience: New York, 1967; pp 312–316.
(21) Sacconi, L.; Midollini, S. *J. Chem. Soc., Dalton Trans.* **1972**, 1213. Figgis, B. N.; Lewis, J. *Prog. Inorg. Chem.* **1964**, *6*, 209.
(22) Bowmaker, G. A.; Boyd, P. D. W.; Campbell, G. K.; Hope, J. M.; Martin, R. L. *Inorg. Chem.* **1982**, *21*, 1152.

acetonitrile as high as 0.1 M had no effect on the cyclic voltammograms of these complexes. For $[Ni(dppm)_2](BF_4)_2$, adding acetonitrile to a nitromethane-d_3 solution of $[Ni(dppm)_2](BF_4)$ to form a 0.1 M solution resulted in a negative shift of the potential of the Ni(II/I) couple by 60 mV and a decrease in the peak to peak separation of this wave. The Ni(I/0) couple shifted approximately 20 mV toward more negative potentials under the same conditions. The observed shifts are consistent with binding of acetonitrile. These results combined with the ^{31}P NMR and electronic absorption spectral results described above indicate $[Ni(dppm)_2](BF_4)_2$ is four-coordinate in nitromethane-d_3 but five-coordinate in the presence of acetonitrile.

In pure acetonitrile the electrochemical behavior for most of the complexes is very similar to that observed in dichloromethane or nitromethane. The two exceptions are $[Ni(dppp)_2](BF_4)$ and $[Ni(dppm)_2](BF_4)_2$. For $[Ni(dppp)_2](BF_4)$ the Ni(II/I) couple is irreversible in acetonitrile. This behavior is similar to that observed for $[Ni(PPh_3)_4]^+$ in acetonitrile, which is oxidized to form $[Ni(PPh_3)_2(CH_3CN)_4]^{2+}$.[11] For $[Ni(dppm)_2(CH_3CN)](BF_4)_2$ in acetonitrile two quasi-reversible waves are observed at high scan rates, i.e., greater than 1 V/s at room temperature or at 50 mV/s at −30 °C. At room temperature and at scan rates of 50 or 100 mV/s these two waves are irreversible and a third cathodic wave is observed at −1.29 V that is not observed in nitromethane. The detailed studies necessary to determine the nature of the chemical reactions following electron transfer are beyond the scope of this work, but under appropriate conditions a good estimate of the half-wave potentials can be obtained.

From Table IV it can be seen that the half-wave potentials for the nickel(II/I) couple becomes more positive as the bite size of the ligand increases. In dichloromethane and nitromethane the potential of the nickel(II/I) couple for $[Ni(dppm)_2](BF_4)_2$ is 0.6 V more negative than that for $[Ni(dppp)_2](BF_4)$. In contrast the half-wave potentials for the I/0 couples are fairly constant, differing by no more than 0.05 V. These observations together with the electronic spectra suggest that the structural features that produce the changes in the potential of the II/I couple occur predominantly in the +2 oxidation state and not in the +1 oxidation state. The structural features of the $[Ni(diphos)_2]^{2+}$ complexes that result in the observed trends for the transition energies shown in Table III and the potentials of the Ni(II/I) redox couples shown in Table IV are the P–Ni–P angle and a concomitant tetrahedral distortion discussed below.

The palladium complexes exhibit reversible or quasi-reversible two-electron reductions with the exceptions of $[Pd(dppm)_2](BF_4)_2$, $[Pd(dppx)_2](BF_4)_2$, and $[Pd(dppp)(PEt_3)_2](BF_4)_2$. The two-electron nature of these redox waves is supported by coulometric measurements, which show that 2.0 ± 0.2 Faradays of charge are passed per mole of complex on reduction, and the observation that the zerovalent complexes $[Pd(dppe)_2]$ and $[Pd(dppp)_2]$ have cyclic voltammograms identical with those of $[Pd(dppe)_2](BF_4)_2$ and $[Pd(dppp)_2](BF_4)_2$. In addition, the peak to peak separation of the waves at 50–100 mV/s are less than 60 mV and approach the 30-mV peak to peak separation expected for a reversible two-electron reduction.[23]

For $[Pd(dppm)_2](BF_4)_2$ the electrochemical reduction is irreversible. The primary electron-transfer step appears to be a two-electron process on the basis of the observation that the ratio of the peak current of the cathodic wave of $[Pd(dppm)_2](BF_4)_2$ to the peak current of the cathodic wave of $[Pd(dppe)_2](BF_4)_2$ is 0.92. The observed half-width of the wave ($E_p - E_{p_{1/2}}$) is 27 mV compared to the 24-mV value expected for a reversible two electron transfer followed by a fast chemical reaction.[24] Controlled-potential coulometry carried out at −1.3 V resulted in the passage of 2.0 Faradays/mol of $[Pd(dppm)_2](BF_4)_2$. A ^{31}P NMR spectrum of the product solution exhibited two resonances at +12.6 and −23.1 ppm, which are assigned to the palladium(0) dimer, $[Pd_2(dppm)_3]$, and dppm, respectively.[25] This data indicates that, following the two-electron reduction of $[Pd(dppm)_2](BF_4)_2$, the resulting palladium(0) complex, $[Pd(dppm)_2]$, undergoes dimerization with loss of dppm. The oxidation wave observed at −0.71 V is assigned to the oxidation of $[Pd_2(dppm)_3]$.

The electrochemical reduction of $[Pd(dppp)(PEt_3)_2](BF_4)_2$ occurs by an irreversible one-electron process. A comparison of the peak height for the reduction wave of $[Pd(dppe)_2](BF_4)_2$ to the wave observed at −0.89 V for $[Pd(dppp)(PEt_3)_2](BF_4)_2$ gives a ratio of 2.77:1. A ratio of 2.54:1 is expected when a reversible two-electron wave is compared to a reversible one-electron wave followed by a fast irreversible reaction, and a ratio of 2.83 is expected for a comparison of a reversible two-electron reduction to a reversible one-electron reduction.[24] Thus, the observed current is consistent with a one-electron process, assuming the diffusion coefficients for these two compounds are similar as would be expected. Controlled-potential electrolysis at −1.2 V vs ferrocene resulted in the passage of 0.85 Faradays/mol of complex. The ^{31}P NMR spectrum of the reduced product exhibited an ABX pattern consistent with the formation of the palladium(I) dimer, **9**, shown in reaction 2. The spectral parameters for this complex

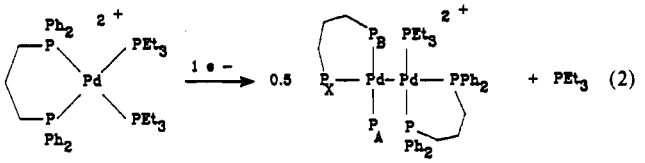

(2)

8 9

are given in Table III. A cyclic voltammogram of the solution produced by bulk electrolysis exhibits no reduction wave at −0.89 V. A reduction wave is observed at −1.48 V and is assigned to the palladium(I) dimer. Oxidation waves at −0.98 and −0.85 V are associated with the reduction at −1.48 V. The waves at −1.48 and −0.85 V are also observed for cyclic voltammograms of $[Pd(dppp)(PEt_3)_2](BF_4)_2$ and decrease with increasing scan rate. These results are consistent with rapid formation of dimer **9** following reduction of $[Pd(dppp)(PEt_3)_2](BF_4)_2$ by one electron.

For $[Pd(dppx)_2](BF_4)_2$ two reversible one-electron reductions are observed in dichloromethane solutions, as shown in Figure 1A. This indicates that the palladium(I) complex, $[Pd(dppx)_2](BF_4)$, is stable with respect to disproportionation. Consistent with this is the observation of a five-line EPR spectrum (Figure 1B) of solutions of $[Pd^I(dppx)_2]^+$ generated by electrochemically reducing $[Pd(dppx)_2]^{2+}$ by one electron. The five-line pattern is attributed to the hyperfine coupling of the four phosphorus atoms of spin $^1/_2$. Although numerous examples of palladium(I) dimers are known, examples of Pd(I) monomers are rare.[10] It is clear that the same structural features that promote the stabilization of monomeric nickel(I) complexes, namely a bidentate phosphine ligand with a large bite, also contribute to the stability of palladium(I) complexes. This would appear to be a general phenomenon, since the increased stability of the rhodium(0) complexes $[Rh(CO)(PPh_3)_3]$ and $[Rh(PPh_3)_4]$ relative to $[Rh(dppe)_2]$ can be understood in terms of stabilization of d^9 complexes with respect to disproportionation by using ligands that permit larger P–M–P angles.[26] It can also be seen from Table IV that increasing the bite size of the diphosphine ligand also leads to a more positive reduction potential just as in the case of the nickel complexes discussed above.

Structural Studies. One of the objectives of the research described in this paper is to establish relationships among the bite size of bidentate phosphine ligands, the structure of their nickel

(23) Bard, A. J.; Faulkner, L. R. *Electrochemical Methods: Fundamentals and Applications*; Wiley: New York, 1980; pp 44–46, 230.
(24) Andrieux, C. P.; Savéant, J. M. In *Investigation of Rates and Mechanisms of Reactions*; Bernasconi, C. F., Ed.; Wiley: New York, 1986; Vol. 6, 41E, Part 2, pp 330–333, 349–350.
(25) Hunt, C. T.; Balch, A. L. *Inorg. Chem.* **1981**, *20*, 2267.
(26) Zotti, G.; Zecchin, S.; Pilloni, G. *J. Organomet. Chem.* **1983**, *246*, 61. Kunin, A. J.; Nanni, E. J.; Eisenberg, R. *Inorg. Chem.* **1985**, *24*, 1852. Mueller, K. T.; Kunin, A. J.; Greiner, S.; Henderson, T.; Kreilick, R. W.; Eisenberg, R. *J. Am. Chem. Soc.* **1987**, *109*, 6313. Pilloni, G.; Zotti, G.; Martelli, M. *Inorg. Chem.* **1982**, *21*, 1284. Keim, W.; Olson, D. C. *Inorg. Chem.* **1969**, *8*, 2028.

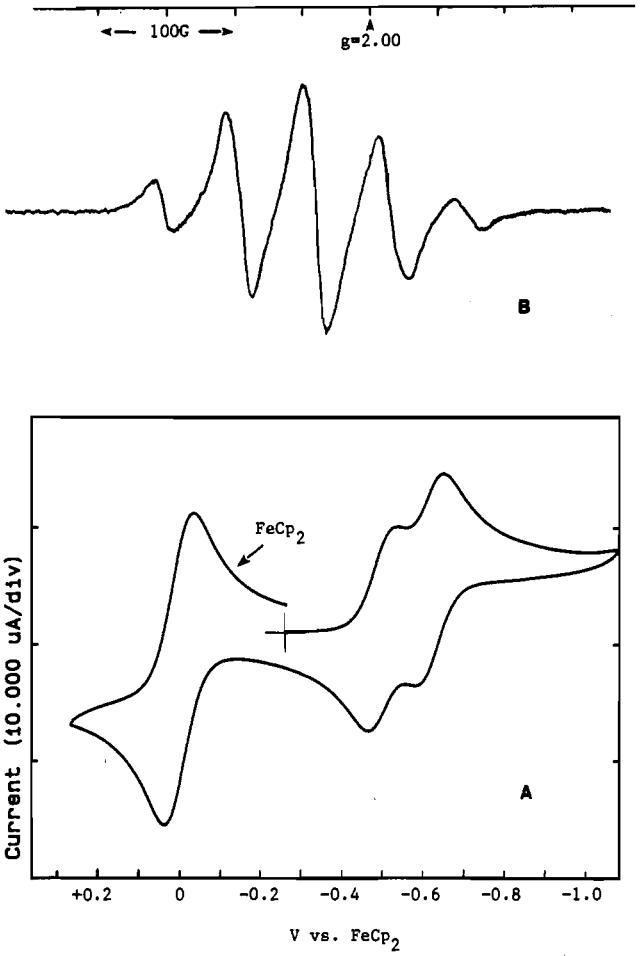

Figure 1. (A) Cyclic voltammogram of a dichloromethane solution containing 1.0×10^{-3} M $[Pd(dppx)_2](BF_4)_2$, ferrocene as an internal standard, and 0.3 N NBu_4BF_4. The scan rate was 40 mV/s. (B) EPR spectrum of the above solution after passing 1.0 Faradays/mol of complex.

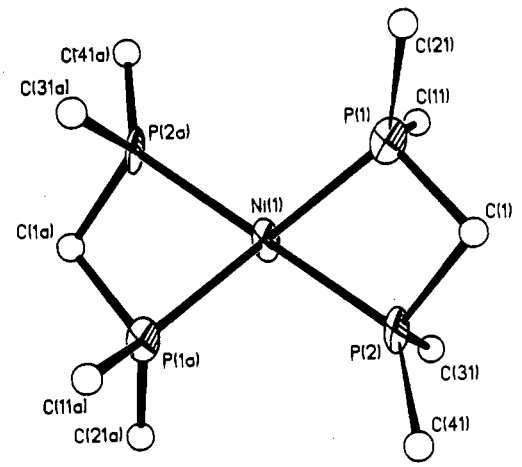

Figure 2. Drawing of the $[Ni(dppm)_2]^{2+}$ cation, showing the atom-numbering scheme.

complexes, and the relative stability of various oxidation states. For nickel complexes containing polyphosphine ligands with methylene, ethylene, *o*-phenylene, and trimethylene linkages, the P–M–P angles formed by the chelating ligand are approximately 73°, 85°,[27] 86°,[28] and 90°,[29] respectively. To complement this series and to provide additional insight into what structural features are most affected by the chelate bite for $[Ni(diphos)_2](BF_4)_2$ complexes, X-ray diffraction studies of $[Ni(dppm)_2](BF_4)_2$ and $[Ni(dppb)_2](PF_6)_2$ have been carried out. Although the structure of $[Ni(dppm)_2](BF_4)_2$ is of low quality due to the quality of the crystals, these studies do provide answers to this basic question.

Orange crystals of $[Ni(dppm)_2](BF_4)_2$ were grown by slow cooling of a hot solution of nitromethane under an atmosphere of nitrogen. The crystals consist of $[Ni(dppm)_2]^{2+}$ cations and BF_4^- anions. The $[Ni(dppm)_2]^{2+}$ cation lies on a crystallographic center of inversion and has approximately C_{2h} local symmetry. One view of the $[Ni(dppm)_2]^{2+}$ cation is shown in Figure 2. Selected bond distances and angles for the $[Ni(dppm)_2]^{2+}$ cation are given in Table V. The average Ni–P distance of 2.22 Å is within the normal range observed for Ni(II) complexes, and the P–C bond distances are normal as well. The small bite size of dppm results in a small P–Ni–P angle of 73.2°. The strain in the four-membered ring is reflected in the P–C–P and Ni–P–C angles of 93.9 and 91.6°, respectively. These values are similar to those observed for *trans*-$[RhHCl(dppm)_2]^+$.[30] In spite of the low quality of the structure, planarity is required by the space group and crystallographic symmetry. The cation lies at a center of inversion, requiring that the NiP_4 core be strictly planar. The planarity of the NiP_4 core means that no tetrahedral distortion is observed for this complex, and the dihedral angle between the two planes defined by the two phosphorus atoms of each dppm ligand and nickel is 0°.

Crystals of $[Ni(dppb)_2](PF_6)_2$ were grown from a mixture of acetonitrile and toluene by cooling at −20 °C. The crystals consist of $[Ni(dppb)]^{2+}$ cations, PF_6^- anions, and toluene solvent molecules. The $[Ni(dppb)_2]^{2+}$ cation has no crystallographically imposed symmetry but has local D_{2d} symmetry. A drawing of the $[Ni(dppb)_2]^{2+}$ cation is shown in Figure 3. Selected bond distances and bond angles for the $[Ni(dppb)_2]^{2+}$ cation are given in

Table V. Selected Bond Lengths (Å) and Angles (deg) for $[Ni(dppm)_2](BF_4)_2$

Bond Distances			
Ni(1)–P(1)	2.219 (8)	Ni(1)–P(2)	2.228 (9)
P(1)–P(2)	2.653 (13)	P(1)–C(1)	1.819 (37)
P(1)–C(11)	1.802 (20)	P(1)–C(21)	1.778 (25)
P(2)–C(1)	1.810 (34)	P(2)–C(31)	1.781 (20)
P(2)–C(41)	1.804 (23)		
Bond Angles			
P(1)–Ni(1)–P(2)	73.2 (3)	Ni(1)–P(1)–C(1)	91.6 (10)
P(2)–Ni(1)–P(1A)	106.8 (3)	Ni(1)–P(1)–C(11)	112.8 (8)
P(2)–Ni(1)–P(2A)	180.0 (1)	C(1)–P(1)–C(11)	106.8 (12)
Ni(1)–P(1)–C(21)	125.5 (7)	C(11)–P(1)–C(21)	107.0 (10)
C(1)–P(1)–C(21)	111.0 (13)	Ni(1)–P(2)–C(1)	91.6 (12)
Ni(1)–P(2)–C(41)	124.2 (7)	Ni(1)–P(2)–C(31)	115.7 (8)
C(1)–P(2)–C(41)	111.2 (13)	C(1)–P(2)–C(31)	106.5 (11)
P(1)–C(1)–P(2)	93.9 (16)	C(31)–P(2)–C(41)	105.7 (11)
P(1)–Ni(1)–P(1A)	180.0 (1)		

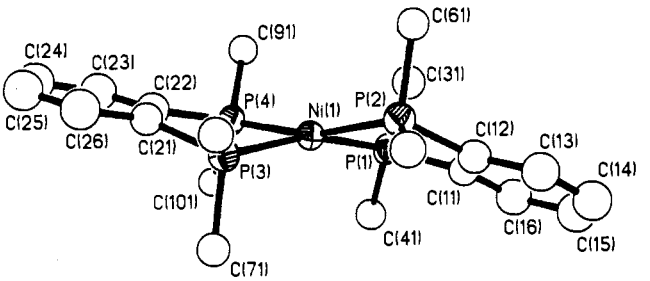

Figure 3. Drawing of the $[Ni(dppb)_2]^{2+}$ cation, showing the atom-numbering scheme.

(27) Hohman, W. H.; Kountz, D. J.; Meek, D. W. *Inorg. Chem.* **1986**, *25*, 616. Di Vaira, M. *J. Chem. Soc., Dalton Trans.* **1975**, 2360. Laneman, S. A.; Stanley, G. G. *Inorg. Chem.* **1987**, *26*, 1177. Orlandini, A.; Sacconi, L. *Inorg. Chem.* **1976**, *15*, 78.

(28) Blundell, T. L.; Powell, H. M. *Acta Crystallogr., Sect. B* **1971**, *B27*, 2304.

(29) Mason, R.; Scollary, G. R.; DuBois, D. L.; Meek, D. W. *J. Organomet. Chem.* **1976**, *114*, C30.

(30) Cowie, M.; Dwight, S. K. *Inorg. Chem.* **1979**, *18*, 1209.

Table VI. Selected Bond Lengths (Å) and Angles (deg) for $[Ni(dppb)_2](PF_6)_2$

Bond Distances			
Ni(1)-P(1)	2.228 (5)	Ni(1)-P(2)	2.218 (6)
Ni(1)-P(3)	2.216 (5)	Ni(1)-P(4)	2.232 (5)
P(1)-C(11)	1.800 (11)	P(1)-C(31)	1.802 (11)
P(1)-C(41)	1.804 (13)	P(2)-C(12)	1.803 (11)
P(2)-C(51)	1.802 (10)	P(2)-C(61)	1.798 (20)
P(3)-C(21)	1.798 (11)	P(3)-C(71)	1.800 (12)
P(3)-C(81)	1.803 (9)	P(4)-C(22)	1.792 (11)
P(4)-C(91)	1.799 (11)	P(4)-C(101)	1.804 (12)

Bond Angles			
P(1)-Ni(1)-P(2)	85.2 (2)	P(1)-Ni(1)-P(3)	163.0 (2)
P(2)-Ni(1)-P(3)	99.0 (2)	P(1)-Ni(1)-P(4)	95.2 (2)
P(2)-Ni(1)-P(4)	164.3 (2)	P(3)-Ni(1)-P(4)	85.2 (2)
Ni(1)-P(1)-C(11)	107.4 (4)	Ni(1)-P(1)-C(31)	119.0 (4)
C(11)-P(1)-C(31)	101.7 (5)	Ni(1)-P(1)-C(41)	113.3 (4)
C(11)-P(1)-C(41)	103.8 (5)	C(31)-P(1)-C(41)	109.8 (5)
Ni(1)-P(2)-C(12)	108.5 (4)	Ni(1)-P(2)-C(51)	125.9 (4)
C(12)-P(2)-C(51)	104.0 (5)	Ni(1)-P(2)-C(61)	104.7 (4)
C(12)-P(2)-C(61)	106.2 (6)	C(51)-P(2)-C(61)	106.1 (5)
Ni(1)-P(3)-C(21)	108.6 (4)	Ni(1)-P(3)-C(71)	101.5 (4)
C(21)-P(3)-C(71)	104.6 (6)	Ni(1)-P(3)-C(81)	128.5 (5)
C(21)-P(3)-C(81)	105.2 (5)	C(71)-P(3)-C(81)	106.3 (5)
Ni(1)-P(4)-C(22)	108.6 (4)	Ni(1)-P(4)-C(91)	111.8 (4)
C(22)-P(4)-C(91)	105.0 (5)	Ni(1)-P(4)-C(101)	121.0 (4)
C(22)-P(4)-C(101)	100.5 (6)	C(91)-P(4)-C(101)	108.3 (5)

Table VII. Structural Data for Four-Coordinate Rhodium(I) and Iridium(I) Phosphine Complexes

compd	α (P-Rh-P angle), deg	β (dihedral angle), deg	ref
$[Rh(dppe)_2](ClO_4)$	82.7	~1	31
$[Rh(dmpe)_2](C_9H_7)$	84.5	0	32
$[Rh(dppbu)_2](BF_4)$[a]	90.2	37, 39	33
$[Rh(PMe_3)_4]Cl$	93.9	42	34
$[Ir\{P(C_6H_5)_2CH_3\}_4](BF_4)$	93.6	40	35

[a] The ligand dppbu is 1,4-bis(diphenylphosphino)butane.

Table VI. The Ni-P bond distances are normal with an average value of 2.22 Å. The P-Ni-P angle of 85.2° formed by the chelating dppb ligand is significantly larger than the 73.2° angle observed for $[Ni(dppm)_2]^{2+}$. The $[Ni(dppb)_2]^{2+}$ cation also exhibits a significant tetrahedral distortion with a dihedral angle between the two planes defined by the two phosphorus atoms of each dppb ligand and nickel of 24.1°. A similar tetrahedral distortion has been observed for a number of "square-planar" rhodium and iridium complexes containing four phosphorus atoms, as shown in Table VII. It is clear from this table that increasing the bite size of the diphosphine ligand results in an increase in the P-Rh-P angle and a larger deviation from a square-planar geometry toward a tetrahedral geometry. This distortion has been attributed to steric interactions between substituents on the phosphine ligands, and in some cases steric repulsions undoubtedly play a major role. However, it is unlikely that the steric contributions to the distortions in $[Rh(PMe_3)_4]^+$ [34] are the same as those in $[Ir(PPh_2Me)_4]^+$,[35] since the cone angles for PMe_3 and PPh_2Me are 118 and 136°, respectively.[36] Steric considerations would also suggest that the dihedral angle for $[Rh(dppe)_2]^+$ should be larger than that for $[Rh(dmpe)_2]^+$; however, both angles are close to zero.[31,32]

As discussed above, the ^{31}P NMR spectra, electronic absorption spectra, and cyclic voltammetry data all indicate coordination of

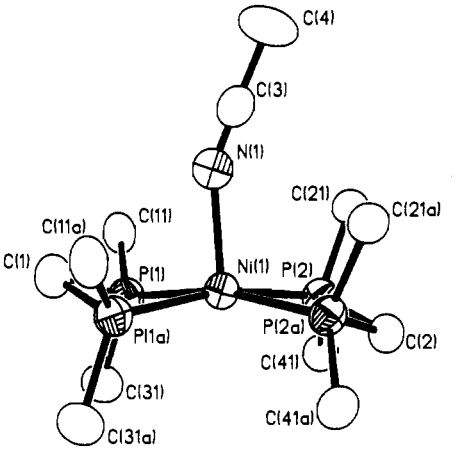

Figure 4. Drawing of the $[Ni(dppm)_2(CH_3CN)]^{2+}$ cation, showing the atom-numbering scheme.

Table VIII. Selected Bond Lengths (Å) and Angles (deg) for $[Ni(dppm)_2(CH_3CN)](PF_6)_2$

Bond Distances			
Ni(1)-N(1)	2.096 (5)	Ni(1)-P(1)	2.222 (1)
Ni(1)-P(2)	2.214 (1)	N(1)-C(3)	1.134 (8)
C(3)-C(4)	1.478 (9)	P(1)-C(1)	1.832 (4)
P(1)-C(11)	1.806 (4)	P(1)-C(31)	1.813 (4)
P(2)-C(21)	1.819 (4)	P(2)-C(2)	1.783 (4)
		P(2)-C(41)	1.811 (4)

Bond Angles			
N(1)-Ni(1)-P(1)	93.4 (1)	P(1)-C(1)-P(1A)	93.0 (3)
P(1)-Ni(1)-P(2)	104.9 (1)	N(1)-Ni(1)-P(2)	99.7 (1)
P(1)-Ni(1)-P(1A)	73.5 (1)	P(2)-N(1)-P(1A)	166.9 (1)
P(2)-Ni(1)-P(2A)	73.7 (1)	N(1)-C(3)-C(4)	177.9 (6)
Ni(1)-N(1)-C(3)	155.7 (5)	Ni(1)-P(1)-C(11)	121.6 (1)
Ni(1)-P(1)-C(1)	91.9 (1)	Ni(1)-P(1)-C(31)	118.9 (2)
C(1)-P(1)-C(11)	110.2 (2)	C(11)-P(1)-C(31)	105.9 (2)
C(1)-P(1)-C(31)	106.1 (2)	Ni(1)-P(2)-C(21)	113.6 (1)
Ni(1)-P(2)-C(2)	93.8 (1)	Ni(1)-P(2)-C(41)	123.3 (1)
C(2)-P(2)-C(21)	109.0 (2)	C(21)-P(2)-C(41)	106.8 (2)
C(2)-P(2)-C(41)	109.0 (2)	P(2)-C(2)-P(2A)	96.3 (3)

acetonitrile to $[Ni(dppm)_2](PF_6)_2$. Recrystallization of this complex from a mixture of acetonitrile and toluene produced crystals of the five-coordinate complex, $[Ni(dppm)_2(CH_3CN)](PF_6)_2$. The crystals are composed of $[Ni(dppm)_2(CH_3CN)]^{2+}$ cations, PF_6^- anions, and a disordered toluene molecule. The cation lies on a crystallographic mirror plane and has local C_{2v} symmetry. A drawing of this molecule is shown in Figure 4, and selected bond distances and angles are given in Table VIII. The geometry of $[Ni(dppm)_2(CH_3CN)]^{2+}$ is clearly square pyramidal with the nickel atom lying 0.25 Å out of the plane defined by the four phosphorus atoms. The equation defining the plane is $6.172x + 18.354y + 0.0z = 9.1285$. The average of the four N-Ni-P bond angles is 96.6°, which is comparable to 96.3° observed for the I-Ni-P angle of $[Ni(TEP)_2I]I$ (TEP is 1,2-bis(diethylphosphino)ethane), which is also square pyramidal.[37] The average Ni-P distance of 2.22 Å is the same as those of $[Ni(dppb)_2]^{2+}$ and $[Ni(dppm)_2]^{2+}$, and the Ni-N bond distance of 2.09 Å is slightly longer than the average bond distance of 2.07 Å observed in high-spin $[Ni(CH_3CN)_6]^{2+}$.[38] An interesting feature of this molecule is the nonlinear coordination of acetonitrile, as reflected by the Ni-N-C angle of 155.5°. The bending seems to be caused by steric interactions between acetonitrile and PF_6^- anions. One PF_6^- anion, which sits on a crystallographic inversion center, makes contacts of 3.18 and 3.42 Å to C(3) and C(4) of the acetonitrile ligand. C(4) also makes a contact of 3.12 Å with

(31) Hall, M. C.; Kilbourn, B. T.; Taylor, K. A. *J. Chem. Soc. A* **1970**, 2539.
(32) Marder, T. B.; Williams, I. D. *J. Chem. Soc., Chem. Commun.* **1987**, 1478-1480.
(33) Anderson, M. P.; Pignolet, L. H. *Inorg. Chem.* **1981**, *20*, 4101.
(34) Jones, R. A.; Real, F. M.; Wilkinson, G.; Galas, A. M. R.; Hursthouse, M. B.; Malik, K. M. A. *J. Chem. Soc., Dalton Trans.* **1980**, 511.
(35) Clark, G. R.; Skelton, B. W.; Waters, T. N. *Acta Crystallogr., Sect. C* **1987**, *C43*, 1708.
(36) Tolman, C. A. *Chem. Rev.* **1977**, *77*, 313.
(37) Alyea, C. E.; Meek, D. W. *Inorg. Chem.* **1972**, *11*, 1029.
(38) Bougon, R.; Charpin, P.; Christie, K. O.; Isabey, J.; Lance, M.; Nierlich, M.; Vigner, J.; Wikon, W. W. *Inorg. Chem.* **1988**, *27*, 138. A table of M-N distances for acetonitrile complexes can also be found in ref 39.
(39) Storhoff, B. N.; Lewis, H. C., Jr. *Coord. Chem. Rev.* **1977**, *23*, 1.

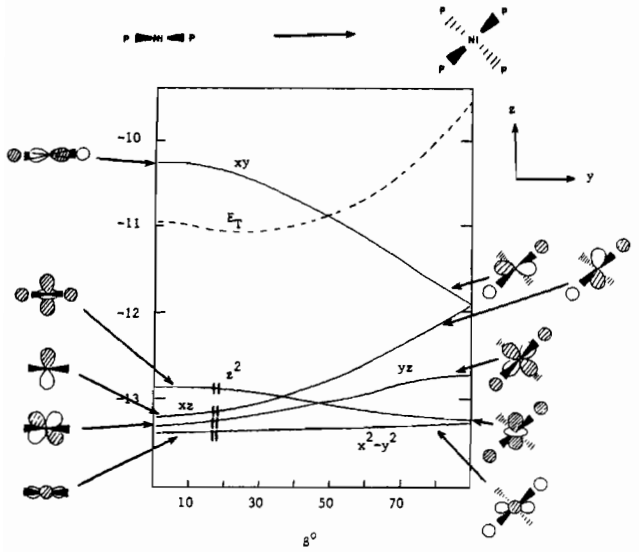

Figure 5. Orbital energies (—) and total energy (---) for $Ni(PH_3)_4^{2+}$ undergoing a distortion from a square-planar geometry (left-hand side) to a tetrahedral geometry (right-hand side). The energy units are in electronvolts.

a second PF_6^- ion, F(51) of P(5).

Molecular Orbital Calculations. In a comparison of the molecular structure of $[Ni(dppm)_2](BF_4)_2$ with that of $[Ni(dppb)_2](PF_6)_2$, two significant structural differences are apparent. First, the P–Ni–P angle, α, is different due to the difference in the bite size of the two ligands. Second, the dihedral angle, β, between the two planes defined by the two phosphorus atoms of the bidentate ligand and nickel increases as the P–Ni–P angle increases. To aid our understanding of the relationship between the chelate angle and the dihedral angle for these complexes, extended Hückel molecular orbital calculations have been carried out for the model compound $[Ni(PH_3)_4]^{2+}$. In the top-left-hand corner of Figure 5 is shown the projection of the $[Ni(PH_3)_4]^{2+}$ molecule as viewed down the x axis for β equal to 0°. The molecule is strictly planar. In the top-right-hand corner is shown the projection of the NiP_4 core for β equal to 90°. This molecule has a fully developed dihedral twist. Figure 5 shows the behavior of the frontier molecular orbitals of $[Ni(PH_3)_4]^{2+}$ as a function of β when α is 85°. On the left-hand side is shown the frontier molecular orbitals of planar $[Ni(PH_3)_4]^{2+}$. These orbitals are those expected for a square-planar metal complex. The totally antibonding dxy orbital lies highest in energy. (This orbital is normally designated as the dx^2-y^2 orbital,[40,41] but in order to maintain a reasonable coordinate system for the "square-planar" to "tetrahedral" distortion, the coordinate system shown in Figure 5 was used. This coordinate system has also been used by other authors.[20]) The dz^2 orbital is lower in energy than in an octahedral complex, since the two antibonding interactions along the z axis have been removed, leaving only those in the xy plane. The largely nonbonding dxz, dyz, and dx^2-y^2 orbitals are lowest in energy.

As $[Ni(PH_3)_4]^{2+}$ is distorted from a planar structure toward a tetrahedral geometry, that is as β increases, the unoccupied dxy orbital drops rapidly in energy as the phosphorus σ orbitals interact less strongly in an antibonding fashion with the dxy orbital of nickel. The filled dz^2 orbital is also stabilized by this distortion, since it results in a reduction of the antibonding interaction of the ligand orbitals with the torus of the dz^2 orbital. The maximum stabilization of the dz^2 orbital occurs for α equal to 109.6° and β equal to 90°, i.e., a tetrahedral geometry. For values of α less than the 85° shown in Figure 5, the stabilization of the dz^2 orbital will be smaller than shown, since for all values of β a significant antibonding overlap between the ligand σ orbitals and the torus of the dz^2 orbital will be observed. Therefore, for small values of α the dz^2 orbital is not as strongly stabilized by the tetrahedral distortion (increasing β) as it is for larger values of α. The dxz orbital is destabilized as it changes from a nonbonding orbital for the planar geometry shown at the left-hand side of Figure 5 to the antibonding orbital shown on the right-hand side of Figure 5. When β is equal to 90°, the dxy and dxz orbitals are required by symmetry to be degenerate. The dyz orbital also rises in energy in a manner similar to the dxz orbital but more gradually, since for α less than 109.6° the phosphorus atoms interact less strongly with the dyz orbital than the dxz orbital. For a tetrahedral geometry the dyz, dxy, and dxz orbitals will be degenerate as will the dx^2-y^2 and dz^2 orbitals. The energy of the dx^2-y^2 is nearly unchanged as β increases, since the rotation of the phosphorus orbitals about the x axis does not significantly alter their overlap with this orbital. It would appear from Figure 5 that if the occupied frontier orbitals dominate the energetics of this molecule, the most stable geometry for a given chelate angle would be determined by a balance between the stabilization of the dz^2 orbital and the destabilization of the xz and yz orbitals produced by increasing the dihedral angle, β. The total energy, E_T, for the orbital occupancy shown is indicated by the dashed curve of Figure 5. It can be seen that the total energy reflects these counterbalancing trends.

Table IX. Comparison of Calculated and Observed Values of β and $E_{1/2}$ as Functions of α

α, deg	73[a]	85[b]	85.4[a]	90[b]
β(calc), deg	0[a]	25	24.1[a]	40
$E_{1/2}$(calc), V	−0.77	−0.56	−0.54	−0.24
$E_{1/2}$(obs), V	−0.70	−0.56[c]	−0.54	−0.12[d]

[a] Experimentally observed values for $[Ni(dppm)_2](BF_4)_2$ and $[Ni(dppb)_2](PF_6)_2$. [b] Values of α are estimated as described in text. [c,d] Experimentally observed half-wave potentials for $[Ni(dppe)_2](BF_4)_2$ and $[Ni(dppp)_2](BF_4)_2$, respectively.

For α equal to 85° an energy minimum is observed for β equal to approximately 25°. This is close to values of 85.4° (α) and 24.1° (β) observed for $[Ni(dppb)_2](BF_4)_2$ described above. A global energy minimum occurs for α equal to 88° and β equal to 39°. The structure of $[Ni(PMe_3)_4]^{2+}$ would therefore be expected to have values of α and β very similar to those observed for $[Rh(PMe_3)_4]^+$ and $[Ir(PPh_2Me)_4]^+$.[34,35] The good agreement between the calculated and observed geometries for the nickel complexes suggests that electronic factors play an important role in the tetrahedral distortions of "square-planar complexes" and that steric contributions are not solely responsible. This is not to say that steric contributions are not important, but electronic contributions may also contribute and should not be neglected.

This qualitative understanding of the relationship between the bite angle, α, of a chelating diphosphine ligand, the dihedral angle, β, and the energies of the frontier orbitals provides a basis for understanding the relationship among α, the redox potentials for the Ni(II/I) couple, and the energy of the lowest energy transition. Table IX lists the calculated the observed values of β and $E_{1/2}$ as a function of α. To make comparisons between calculated and observed values of $E_{1/2}$, values for α of 85 and 90° were used for $[Ni(dppe)_2](BF_4)_2$ and $[Ni(dppp)_2](BF_4)_2$, respectively. These values are consistent with literature structural data.[27,29] β(calc) is the value of β that gives the minimum energy for each value of α. The calculated half-wave potentials are based on the energy of the lowest unoccupied molecular orbital for the geometry defined by α and β(calc). The value of the lowest unoccupied molecular orbital is normalized to the experimental values by arbitrarily setting the calculated energy of lowest occupied molecular orbital of $[Ni(PH_3)_4]^{2+}$ (for α equal to 85.4° and β equal to 24.1°) equal to the $E_{1/2}$ value observed for $[Ni(dppb)_2](PF_6)_2$. It can be seen that the observed and calculated values of $E_{1/2}$ agree reasonably well. Given the level of sophistication of the extended Hückel method and the uncertainty of α and β, the calculated values for the half-wave potentials are not expected to agree quantitatively with the observed values. It is reassuring, however, to observe that the calculated values of $E_{1/2}$ vary with α in the same qualitative manner as the experimental values.

(40) Cotton, F. A. *Chemical Applications of Group Theory*, 2nd ed.; Wiley-Interscience: New York, 1971; p 269.
(41) Burdett, J. K. *Molecular Shapes*; Wiley: New York, 1980; p 141.

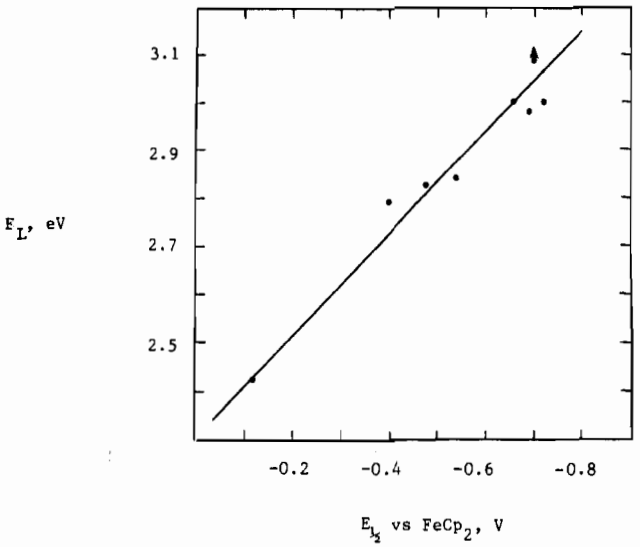

Figure 6. Plot of the lowest transition energies, E_L (from Table III in electronvolts), vs the half-wave potentials for the Ni(II/I) couples from Table IV.

If the energy of the highest occupied molecular orbital varies less strongly with α than the energy of the lowest unoccupied molecular orbital, then the energy of the lowest energy transition should depend largely on the energy of the lowest occupied molecular orbital just as the reduction potential, $E_{1/2}$, depends on the energy of this orbital. It can be seen from Figure 5 that the energy of the highest occupied molecular orbital is much less dependent on α than is the energy of the lowest unoccupied molecular orbital. It is expected then that an approximately linear relationship should exist between the lowest energy electronic transition, E_L, and the half-wave potential of the Ni(II/I) couple. A plot showing this relationship is shown in Figure 6. It can be seen that a reasonable correlation does exist between these data, as expected.

By an extension of the ideas developed above, the increasing stability of the nickel(I) complexes with increasing bite size can be understood as well as the stability of the mononuclear palladium(I) complex, $[Pd(dppx)_2](BF_4)$. The tetrahedral distortions of the nickel and palladium complexes increase as the bite size of the ligands increase due to the stabilization of the dz^2 orbital and steric repulsions. The Ni(II/I) and Pd(II/I) couples are shifted in a positive direction as a result of the stabilization of the dxy orbital. For palladium, the II/I couple for ligands with two- and three-carbon linkages lies negative of the I/0 couple. However, for $[Pd(dppx)_2](BF_4)_2$ the dxy orbital has been sufficiently stabilized that the II/I couple occurs at potentials positive of the I/0 couple. It should be possible to prepare other stable palladium(I) complexes by using bidentate phosphine ligands with large bites. The qualitative correlation between increasing α and β and an increased stability of d^9 metal complexes to disproportionation should be general. It accounts for the increased stability of the nickel(I) and palladium(I) complexes described in this paper and the stability of other d^9 complexes.[26]

Summary and Discussion

In this paper we have described the synthesis and characterization of several four-coordinate nickel(II) and palladium(II) complexes containing diphosphine ligands. Complexes containing two different ligands have also been prepared and characterized. For the nickel complexes the half-wave potential of the II/I couple becomes more positive and the energy of the lowest energy electronic transition decreases as the bite size of the diphosphine ligand increases. These observations resulted in the isolation of a very stable nickel(I) complex, $[Ni(dppp)_2](BF_4)$, and the electrochemical generation of a stable palladium(I) complex, $[Pd(dppx)_2](BF_4)$. Structural studies of $[Ni(dppm)_2](BF_4)_2$ and $[Ni(dppb)_2](PF_6)_2$ indicate that an increase in the bite size of the diphosphine ligands is accompanied by a tetrahedral distortion.

Table X. Extended Hückel Parameters

atom	orbital	H_{ij}, eV	ζ_1	ζ_2	C_1[a]	C_2[a]
H	1s	−13.6	1.30			
P	3s	−18.60	1.60			
	3p	−14.00	1.60			
	3d	−7.00	1.40			
Ni	4s	−8.86	2.10			
	4p	−4.90	2.10			
	3d	−12.99	5.75	2.00	0.5683	0.6292

[a] Coefficient used in double-ζ expansion of d orbitals.

Molecular orbital calculations for the model compound $[Ni(PH_3)_4]^{2+}$ indicate that this tetrahedral distortion has an electronic origin in addition to the more commonly invoked steric contribution.

The results summarized in the preceding paragraph suggest two main conclusions. First, it is not correct to assume in all cases that four-coordinate diamagnetic d^8 metal complexes prefer a square-planar geometry. In fact for d^8 nickel complexes containing four phosphine ligands, electronic factors appear to favor a strongly distorted geometry with a bite angle of ~90° and a dihedral angle of ~40°. The energy surface is fairly soft, and a variety of structures can be expected as steric and electronic forces reach a compromise. The second important conclusion to be drawn from these studies is that irregardless of their origin, the experimentally observed tetrahedral distortions have a major influence on the electronic structure of these molecules. This distortion results in the stabilization of the lowest unoccupied molecular orbital of these complexes. This is reflected in the observation that the half-wave potentials of the Ni(II/I) couples for $[Ni(dppm)_2](BF_4)_2$ and $[Ni(dppp)_2](BF_4)$ differ by 0.6 V. The stabilization of the lowest unoccupied molecular orbital results in a much wider potential range for which Ni(I) and Pd(I) complexes are stable. For $[Ni(dppp)_2](BF_4)$ the +1 oxidation state is stable over a potential range of approximately 0.8 V. In contrast, $[Ni(dppe)_2](BF_4)$ is stable over a potential range of only 0.2–0.3 V. By extending these ideas to palladium, it is possible to generate an unusual monomeric Pd(I) species, $[Pd(dppx)_2](BF_4)$, by using a ligand with a large bite. These same principles should be applicable to other metals as well.

Another interesting observation is the coordination of acetonitrile to the nickel complexes containing dppm as a ligand. As discussed in the section on molecular orbital calculations, the dz^2 molecular orbital is not appreciably stabilized by a tetrahedral distortion because of the small bite of this diphosphine ligand. A distortion that will stabilize this orbital is the downward movement of all four phosphorus ligands with respect to nickel. This will also result in the formation of a low-lying vacant hybrid orbital appropriate for coordination of a fifth ligand. This is precisely what is observed for $[Ni(dppm)_2](BF_4)_2$, $[Ni(dppm)(dppe)](BF_4)_2$, and $[Ni(dppm)(dppp)](BF_4)_2$. It is interesting to note that $[Pt(dppm)_2]^{2+}$ readily forms five-coordinate complexes as well.[42] The above results suggest attributing differences in reactivity patterns to differences in ring strain is an oversimplification. Attention needs to be given to the electronic effects occurring at the metal that result from the change in the bite size of chelating ligands.

Appendix

Extended Hückel calculations[43] were performed by using the weighted H_{ij} formula.[44] The atomic parameters are listed in Table X with the nickel parameters taken from ref 45. A double-ζ expansion was used for the d orbitals of nickel.

(42) Grossel, M. C.; Moulding, R. P.; Seddon, K. R.; Walker, F. J. *J. Chem. Soc., Dalton Trans.* **1987**, 705.
(43) Hoffmann, R. *J. Phys. Chem.* **1963**, *39*, 1397. Hoffmann, R.; Lipscomb, W. N. *Ibid.* **1962**, *36*, 3179.
(44) Ammeter, J. H.; Bürgi, H. B.; Thibeault, J. C.; Hoffmann, R. *J. Am. Chem. Soc.* **1978**, *100*, 3686.
(45) Hoffman, D. M.; Hoffmann, R.; Fisel, C. R. *J. Am. Chem. Soc.* **1982**, *104*, 3858.

Acknowledgment. This work was supported by the United States Department of Energy, Office of Basic Energy Sciences, Chemical Sciences Division.

Supplementary Material Available: For $[Ni(dppm)_2](BF_4)_2$, $[Ni(dppb)_2](BF_4)_2$, and $[Ni(dppm)(CH_3CN)](PF_6)_2$, Entries 1s–3s, containing text describing X-ray crystallographic experimental procedures, Figures 1s–3s, showing thermal ellipsoid plots with numbering schemes, and Tables 1s–6s, 8s–13s, and 15s–20s, listing atomic coordinates and equivalent isotropic displacement parameters, bond lengths, bond angles, anisotropic displacement parameters, and hydrogen atom coordinates and isotropic displacement parameters (41 pages); Tables 7s, 14s, and 21s, listing calculated and observed structure factors (32 pages). Ordering information is given on any current masthead page.

Contribution from the Anorganisch-Chemisches Institut, Universität Münster, D-4400 Münster, West Germany

Sc_3C_4, a Carbide with C_3 Units Derived from Propadiene

Rainer Pöttgen and Wolfgang Jeitschko*

Received June 14, 1990

The title compound was prepared in well-crystallized form by annealing the elemental components in a palladium matrix slightly below the melting point of palladium. It crystallizes in the tetragonal space group *P4/mnc* with the lattice constants a = 748.73 (5) pm, c = 1502.6 (2) pm, and Z = 10 formula units per cell. The structure was determined from single-crystal X-ray data and refined to R = 0.019 for 476 structure factors and 35 variable parameters. It is the first well-characterized carbide containing C_3 units (eight per cell). In addition, two C_2 pairs and twelve isolated carbon atoms per cell are present. The C–C bond lengths in the nearly linear (176°) C_3 units (2 × 134 pm) and in the C_2 pairs (125 pm) correspond to double and nearly triple bonds, respectively. The compound may therefore be considered as a derivative of allene, ethyne, and methane. The C_3 units are coordinated to ten scandium atoms, forming bicapped quadratic antiprisms. The C_2 pairs and the isolated carbon atoms have octahedral scandium environments. Sc_3C_4 is a metallic conductor and a Pauli paramagnet. This is qualitatively rationalized by chemical bonding considerations. The compound was previously described with the tentative composition "$Sc_{15}C_{19}$" by Jedlicka, Nowotny, and Benesovsky (*Monatsh. Chem.* **1971**, *102*, 389). The compounds R_3C_4 (R = Ho–Lu) are isotypic with Sc_3C_4. The corresponding yttrium compound could only be obtained by adding 5 atom % boron to the samples.

Introduction

The well-known salt-like carbide Al_4C_3 and the technically important carbides of the transition metals contain isolated carbon atoms. C_2 pairs are known to occur in CaC_2 and in the carbides of the rare-earth elements R_2C_3 and RC_2.[1] More recently C_2 pairs were found in many ternary carbides of the rare-earth elements with transition metals.[2] The hydrolyses of these and other carbides frequently result in gaseous products containing large amounts of C_3, C_4, C_5, and C_6 hydrocarbons.[3] In no case, however, could it be shown by structure determinations that such higher carbon units are present in the solid. Thus, Sc_3C_4 is the first well-characterized carbide containing C_3 units. We obtained a well-crystallized sample of Sc_3C_4 during an investigation of the ternary system scandium–palladium–carbon. In contrast, from binary samples we have only obtained polycrystalline Sc_3C_4. A structure proposal for this phase was made on the basis of X-ray film data of a poor-quality crystal some 20 years ago.[4] It resulted in the tentative composition "$Sc_{15}C_{19}$". This composition was assumed to be correct in all subsequent investigations of this phase[5] and the isotypic rare-earth carbides.[6–9]

Sample Preparation and Lattice Constants of Sc_3C_4

Starting materials were scandium chips (>99.9%, no visible contamination by scandium oxide) and graphite flakes (>99.5%). Cold-pressed pellets of the ideal composition were melted in an arc-melting furnace in an argon (99.996%) atmosphere. The argon was further purified by repeatedly melting a titanium button prior to the reaction. The samples were then wrapped in tantalum foil and annealed in silica tubes for 3 weeks at 900 °C. The Guinier powder patterns of these samples showed single-phase Sc_3C_4. The single crystals used for the structure determination were obtained from a sample containing palladium (>99.9%) with the atomic proportions Sc:Pd:C = 2:1:2. After arc-melting, the sample was annealed in an evacuated, sealed, water-cooled silica tube in a high-frequency furnace 8 h at a temperature slightly below the melting point of the palladium matrix. The single crystals of Sc_3C_4 were isolated from the crushed button, which was kept under dried paraffin oil. The Guinier powder pattern of this sample showed Sc_3C_4 as the main phase besides small amounts of $ScPd_3$ and graphite. Energy-dispersive analyses in a scanning electron microscope did not reveal any contamination of the crystals by palladium.

Table I. Crystallographic Data for Sc_3C_4

sp gr: *P4/mnc* (No. 128)	ρ_{calc} = 3.606 g·cm^{-3}
a = 748.73 (5) pm	μ = 56.4 cm^{-1}
c = 1502.6 (2) pm	transm ratio (highest/lowest): 1.12
V = 0.8424 (2) nm^3	R_i = 0.071
Z = 10	$R(F_o)$ = 0.019
fw = 182.91	$R_w(F_o)$ = 0.018
T = 21 °C	$w = 1/\sigma^2$
λ = 0.7107 Å	

The lattice constants of Sc_3C_4 (Table I) were obtained from the binary sample with the Guinier technique using Cu $K\alpha_1$ radiation and α-quartz (a = 491.30 pm, c = 540.46 pm) as a standard. The identification of the diffraction lines was facilitated by intensity calculations[10] using the positional parameters of the refined structure. The lattice constants of Sc_3C_4 determined on the four-circle diffractometer were in good agreement with those obtained from the powder.

Properties

Crystals of Sc_3C_4 have a light gray color with metallic luster; powdered samples are black. They react readily with the humidity of the air; microcrystalline samples are completely decomposed after some hours. The gaseous products of the hydrolyses of "$Sc_{15}C_{19}$" samples under different conditions were analyzed previously by gas chromatography.[5] The amounts of the C_1, C_2, and C_3 hydrocarbons obtained agree approximately with those expected from the crystal structure, although minor amounts of higher hydrocarbons were also found.

(1) Atoji, M.; Gschneidner, K., Jr.; Daane, A. H.; Rundle, R. E.; Spedding, F. H. *J. Am. Chem. Soc.* **1958**, *80*, 1804. Spedding, F. H.; Gschneidner, K., Jr.; Daane, A. H. *J. Am. Chem. Soc.* **1958**, *80*, 4499.
(2) Hoffmann, R.-D.; Jeitschko, W.; Boonk, L. *Chem. Mater.* **1989**, *1*, 580.
(3) Jeitschko, W.; Gerss, M. H.; Hoffmann, R.-D.; Lee, S. *J. Less-*Common *Met.* **1989**, *156*, 397.
(4) Jedlicka, H.; Nowotny, H.; Benesovsky, F. *Monatsh. Chem.* **1971**, *102*, 389.
(5) Hâjek, B.; Karen, P.; Brožek, V. *J. Less-Common Met.* **1984**, *96*, 35.
(6) Bauer, J.; Nowotny, H. *Monatsh. Chem.* **1971**, *102*, 1129.
(7) Bauer, J. *J. Less-Common Met.* **1974**, *37*, 161.
(8) Bauer, J.; Bienvenu, H. *C. R. Seances Acad. Sci. Ser. C* **1980**, *290*, 387.
(9) Bauer, J.; Ansel, D. *J. Less-Common Met.* **1985**, *109*, L9.
(10) Yvon, K.; Jeitschko, W.; Parthé, E. *J. Appl. Crystallogr.* **1977**, *10*, 73.

0020-1669/91/1330-0427$02.50/0